ChemComm

Accepted Manuscript

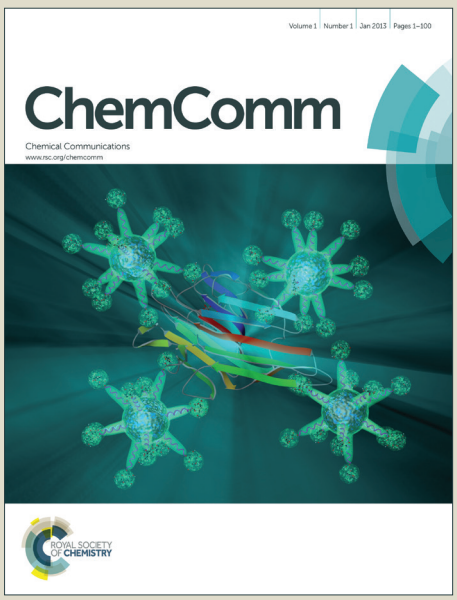

ROYAL SOCIETY OF CHEMISTRY

www.rsc.org/chemcomm

Journal Name

RSCPublishing

COMMUNICATION

New Members of Layered Oxychloride Perovskites with Square Planar Coordination: $Sr_2MO_2Cl_2$ (M = Mn, Ni) and $Ba_2PdO_2Cl_2$

Cite this: DOI: 10.1039/x0xx00000x

Received 00th January 2012,
Accepted 00th January 2012

DOI: 10.1039/x0xx00000x

www.rsc.org/

Y. Tsujimoto[a] C. I. Sathish[b] Y. Matsushita[c] K. Yamaura[b] and T. Uchikoshi[a]

New members of Ruddlesden-Popper type layered oxychloride compounds, $Sr_2MO_2Cl_2$ (M = Mn, Ni) and $Ba_2PdO_2Cl_2$, were synthesized under high-pressure conditions. Synchrotron XRD analysis revealed that all the phases adopt the tetragonal space group *I*4/*mmm*, where two-dimensional sheets composed of corner-sharing MO_4/PdO_4 squares were separated by rock-salt SrCl/BaCl layers.

Among many types of coordination geometries, square planar coordination has particularly received considerable attention from the perspective of superconductivity and low-dimensional magnetism.[1] $Sr_2CuO_2Cl_2$ is not only an ideal two-dimensional (2D) quantum Heisenberg antiferromagnet but also a parent compound of high-T_c superconductors.[2] $Sr_2CuO_2Cl_2$ is a Ruddlesden-Popper (R-P) type layered perovskite with the tetragonal K_2NiF_4 structure (space group *I*4/*mmm*).[3] As shown in Fig. 1 (a), the CuO_2 plane is alternately stacked with double rock-salt SrCl layers along the *c* axis. More specifically, the copper atom is loosely bound to the apical halogen atoms, but the copper coordination geometry can be viewed as a CuO_4 square due to the significantly elongated Cu–Cl bonds. The crystal symmetry is maintained down to low temperatures,[3] in sharp contrast to isostructural compounds (*T*-type) La_2CuO_4 and K_2CuF_4 showing an orthorhombic distortion below 530 K[4] and an cooperative orbital ordering of $d(x^2–r^2)/d(y^2–r^2)$[5], respectively. To date, many kinds of layered oxyhalide compounds analogous to R-P type structure have been reported; however, the variety of elements in square planar coordination is limited to Cu(II) with Jahn-Teller (J-T) effects and Pd(II) in a low-spin d^8 configuration with large crystal-field splitting energy.[6, 7, 8] Nevertheless, recent developments in synthetic methods successfully extended oxychloride systems with square-planar coordination to $Sr_2Co^{2+}O_2X_2$ (X = Cl, Br)[9] and $Sr_3M_2O_4Cl_2$ (M^{2+} = Fe, Co)[10] analogous to $Sr_2CuO_2Cl_2$ and $Ca_3Cu_2O_4Cl_2$[7], respectively.

High-pressure synthesis is a very useful technique to obtain new metastable phases that cannot be formed by conventional solid-state reaction. We recently synthesized new oxyhalide compounds Sr_2CoO_3F and Sr_2NiO_3X (X = F, Cl),[11] where the transition metal centres are surrounded with four oxygen at the equatorial sites and halogen/oxygen atoms at the apical sites (Fig. 1(c)). Similarly to $Sr_2CuO_2Cl_2$, these compounds have weak interaction between the transition metal centre and the halide ion, leading to formation of a distorted square pyramid with the surrounding oxide ions.[12] As seen in $Sr_2CoO_2Cl_2$ and Sr_2CoO_3Cl, full filling of apical sites with halide ions allows to change coordination environment around the metal centre from square pyramid to square plane.[9, 13] However, only two examples are known in the $Sr_2MO_2Cl_2$ (M = Co, Cu) family until now, which hampers systematic study of the 2D magnetism as a function of quantum spin number. Thus, preparation of another members of this family are highly demanded.

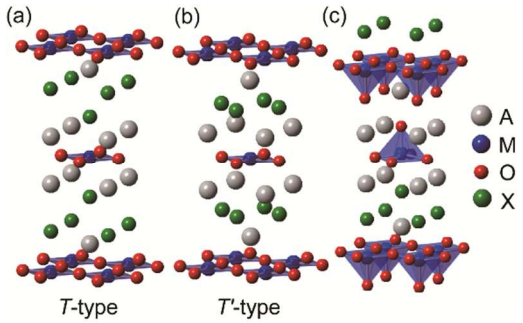

Fig. 1 Crystal structure of (a, b) $A_2MO_2X_2$ and (c) A_2MO_3X (A = rare earth, Alkali, Alkaline earth metal; M = transition metal; X = halogen).The structures of (a) and (b) are termed *T*-(La_2CuO_4) and *T*′-(Nd_2CuO_4) phases, respectively.

In this communication, we report new members of layered oxychloride compounds with a square planar coordination, $Sr_2MnO_2Cl_2$, $Sr_2NiO_2Cl_2$ and $Ba_2PdO_2Cl_2$, which are isostructural with $Sr_2CuO_2Cl_2$. All the present compounds were synthesized by a high-pressure and high-temperature method. Magnetic susceptibility measurements for the three compounds revealed characteristic magnetism reflecting their electronic structures: paramagnetic, antiferromagnetic (AFM) and diamagnetic behaviours for the manganese, nickel and palladium oxychloride compounds, respectively.

$Sr_2MnO_2Cl_2$, $Sr_2NiO_2Cl_2$ and $Ba_2PdO_2Cl_2$ were prepared from stoichiometric mixtures of in-house synthesized SrO_2, Mn (99.9 %)

and $SrCl_2$ (99.9%), SrO_2, Ni (99.9%) and $SrCl_2$, and BaO (99%), PdO (99.9%) and $BaCl_2$ (99.9%), respectively. Each mixture enclosed in a Pt capsule was heated for 1 h in a belt-type high-pressure apparatus at 3 GPa and 1400 °C for $Sr_2NiO_2Cl_2$ and $Ba_2PdO_2Cl_2$, and at 6 GPa and 1500 °C for $Sr_2MnO_2Cl_2$. After the treatment, the samples were quickly quenched to room temperature, and then the pressure was slowly released. The sample colour were black for $Sr_2MnO_2Cl_2$ and $Ba_2PdO_2Cl_2$, and dark green for $Sr_2NiO_2Cl_2$. Synchrotron powder X-ray diffraction (SXRD) data were collected at room temperature using a one-dimensional X-ray detector installed on BL15XU,[14] NIMS beamline at SPring-8. The wave length was λ = 0.65298 Å. The data were analysed by the Rietveld method with the program RIETAN-FP.[15] Magnetic susceptibilities were measured over the temperature range of T = 10−400 K in an applied magnetic field of H = 1 kOe for $Sr_2MnO_2Cl_2$ and $Sr_2NiO_2Cl_2$ and H = 10 kOe for $Ba_2PdO_2Cl_2$, using a superconducting quantum interference device (SQUID) magnetometer (Quantum Design, MPMS-XL).

Table. 1. Crystallographic data for $Sr_2MO_2Cl_2$ (M = Mn, Ni) and $Ba_2PdO_2Cl_2$ from Rietveld refinement of synchrotron X-ray diffraction data.

		$Sr_2MnO_2Cl_2$		$Sr_2NiO_2Cl_2$		$Ba_2PdO_2Cl_2$	
Atom	Site	z	B_{iso} (Å)	z	B_{iso} (Å)	z	B_{iso} (Å)
Sr/Ba	(0,0,z) 4*e*	0.38753(10)	1.93(3)	0.39320(7)	0.85(2)	0.38764(3)	0.667(9)
M	(0,0,0) 2*a*	–	1.82(8)	–	0.71(5)	–	0.315(13)
O	(0,1/2,0) 4*c*	–	0.2(1)	–	1.40(12)	–	0.81(7)
Cl	(0,0,z) 4*e*	0.1834(2)	0.76(6)	0.17994(17)	0.78(6)	0.18816(11)	1.03(2)
a (Å)		4.09669(2)		4.03896(4)		4.12886(1)	
c (Å)		14.99435(16)		15.09293(16)		16.80766 (4)	
R_{wp} (%)		1.56		1.46		4.25	
R_g (%)		7.65		5.63		3.13	
S		2.11		1.63		2.54	
M–O (Å)		2.04835(1)		2.01948(3)		2.06443(1)	
M–Cl (Å)		2.750(5)		2.716(3)		3.1625(19)	
Sr/Ba–O (Å)		2.6535(10)		2.5839(7)		2.7979(4)	
Sr/Ba–Cl×2 (Å)		3.0857(17), 3.060(5)		3.0619(11), 3.219(3)		3.1854(8), 3.353(2)	

Figures 2(a)−(c) show the SXRD patterns of $Sr_2MnO_2Cl_2$, $Sr_2NiO_2Cl_2$ and $Ba_2PdO_2Cl_2$, respectively. All the data could be readily indexed on the simple body-centred tetragonal cell. Close inspection of the data revealed a small number of tiny and broad additional peaks, which are likely assigned as impurity phases. The lattice parameters of the products are a = 4.09669(2) Å and c = 14.99435(16) Å for $Sr_2MnO_2Cl_2$, a = 4.03896(4) Å and c = 15.092923(16) Å for $Sr_2NiO_2Cl_2$, a = 4.12886(1) Å and c = 16.80766(4) Å for $Ba_2PdO_2Cl_2$. Structural refinements based on a model of $Sr_2CuO_2Cl_2$ (space group $I4/mmm$) immediately converged well. The refined crystallographic data, including the atomic coordinates, isotropic atomic displacement parameters (B_{iso}) and selected bond lengths are presented in Table 1.

Common to all the products, the transition metal centre is surrounded with four oxide ions at the equatorial sites and two chloride ions at the apical sites. However, the coordination environment of the transition metal centres can be viewed as a square plane within the 1st coordination sphere. For example, the inplane Mn−O bond length (2.0483 Å) agrees well with the sum of the ionic radii of O^{2-} (r = 1.4 Å) and Mn^{2+} in four-fold coordination (r = 0.66 Å), rather than in six-fold coordination (r = 0.83 Å).[16] In addition, the Mn−Cl bonds (2.750 Å) along the c axis are much longer than those expected from the simple ionic model. The bond ratio of Mn−Cl/Mn−O is 1.34, comparable to the corresponding value of 1.35 for $Sr_2CoO_2Cl_2$, but smaller than 1.44 for $Sr_2CuO_2Cl_2$ with a strong J-T active Cu^{2+} centre. Bond valence sums (BVS) calculated for the manganese site is 2.36, consistent with the nominal oxidation state of Mn(II). It is worth noting that contribution of the Mn−Cl bonds to the total BVS for the manganese is only 15%. Therefore, we can conclude that the manganese coordination is effectively square planar. Same is true for the nickel and palladium oxychlorides with the bond ratios of 1.34 and 1.53. The BVS values for the nickel and palladium sites are 1.77 and 2.01, and the contributions of Ni−Cl and Pd−Cl bonds to the total BVS for the transition metal centre are 16.8% and 4.8%. The larger bond ratio and weaker Pd−Cl apical interaction in $Ba_2PdO_2Cl_2$ than those in $Sr_2MO_2Cl_2$ (M = Mn, Ni) can be explained by the general trend that the crystal field energy is larger in 4*d* series than that in 3*d* series. In fact, the large crystal-field splitting between $4d_{xy}$ and $4d_{x^2-y^2}$ orbitals of Pd(II) exclusively gives the formation of four coplanar bonds, accompanied by a low-spin configuration with S = 0.[8, 17] Similarly, the isoelectronic configuration would be expected for the d^8 nickel centre in $Sr_2NiO_2Cl_2$; however, this is not the case because relatively weak crystal field of Ni(II) in the nickel oxychloride creates half-filled d_{xy} and $d_{x^2-y^2}$ orbitals, that is, a high-spin state with S = 1, as presented later.

The newly obtained oxychloride compounds crystallize in the T (La_2CuO_4) type structure, which is significantly different from related oxyfluoride compounds such as $Sr_2CuO_2F_2$ and $Ba_2PdO_2F_2$, with the T' (Nd_2CuO_4) type structure (Fig. 1(b)).[8, 18] In a series of Ln_2CuO_4 (Ln = lanthanide), a transformation from T to T' structure takes place with smaller Ln^{3+} cations than La^{3+}.[19] Our structural studies suggest that the ionic size of halide ion is also a key factor to affect the relative stabilities of the two structures. In fact, related oxychlorides/oxyfluorides exclusively adopt the T/T'-type structure. There is one exception that $Sr_2CuO_2F_{2+\delta}$, where fluorine atoms are additionally located in the apical sites, adopts the T structure.[20] The structural transformation is induced by a change in anion stoichiometry.

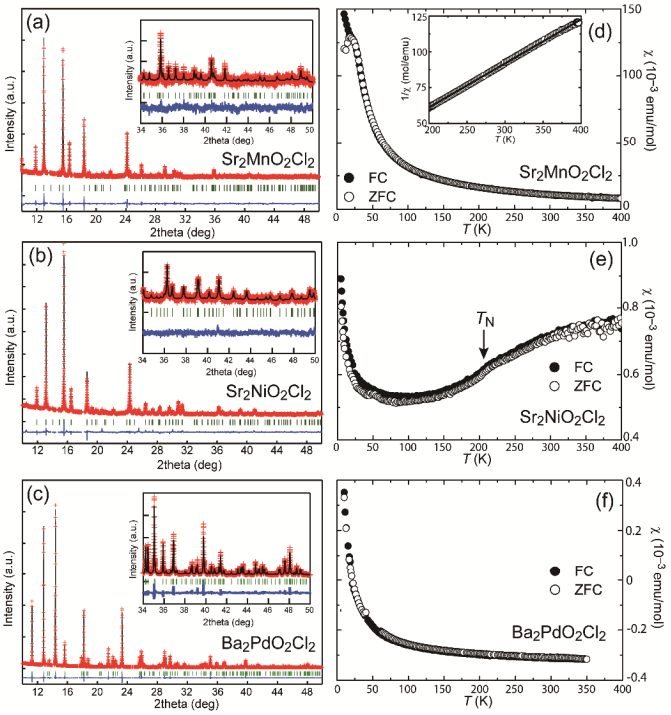

Fig. 2 (a)−(c) Observed (crosses), calculated (upper solid line), and difference (bottom solid line) plots from the Rietveld structural refinements against the synchrotron X-ray diffraction data collected from $Sr_2MnO_2Cl_2$, $Sr_2NiO_2Cl_2$ and $Ba_2PdO_2Cl_2$ at room temperature. Bragg reflections are indicated by vertical lines. The inset is a magnified view in a high 2θ region. (d)−(f) Magnetic susceptibilities (χ) measured under zero field cooled (open circles) and field cooled (solid circles) conditions. The inset shows the inverse susceptibility (open circles) and Curie-Weiss fit (solid line).

Figures 2(d)−(f) show the temperature dependence of the magnetic susceptibilities χ (= M/H) of the present compounds,

measured under zero-field cooled (ZFC) and field cooled (FC) conditions. The χ–T curve of $Ba_2PdO_2Cl_2$ shown in Fig. 2(f) exhibited a diamagnetic behaviour, indicating a d^8 low-spin configuration of Pd(II). A paramagnetic increase on cooling should be attributed to impurities or defects in the PdO_2 plane. In contrast, $Sr_2NiO_2Cl_2$, as shown in Fig. 2(e), displayed positive values over the measured temperature range and a gradual drop with decreasing temperatures from 400 K, indicative of 2D AFM correlation in the NiO_2 plane. The χ appears to take a maximum value at around 400 K ($\approx T^{\chi}_{max}$). In addition, a tiny cusp visible at T_N = 210 K is likely caused by a long-range magnetic ordering. Here, it is interesting to compare with a typical 2D antiferromagnet K_2NiF_4 with octahedrally coordinated nickel cations (T^{χ}_{max} = 250 K and T_N = 110 K).[21] The larger value of T^{χ}_{max} in the oxychloride underlies stronger superexchange interactions between the nearest neighbour nickel ions, which likely results from the square planar coordination of the nickel centre enhancing the orbital hybridization between nickel and ligands. Similarly to the nickel oxychloride, the manganese counterpart is expected to have AFM interactions within the MnO_2 plane. However, no sign of a long-range magnetic ordering was found in the χ of $Sr_2MnO_2Cl_2$ (Fig. 2(d)). Instead, it showed a paramagnetic behaviour down to 16 K, accompanied by a hysteresis between the ZFC and FC data. The Curie-Weiss fit to the data between 200 and 400 K gave C = 3.24 emu K/mol and θ = 1.5 K, where C and θ represent Curie constant and Weiss temperature, respectively. The estimated C value is much lower than a spin only value (4.37 emu K/mol) expected for Mn(II) in the high-spin configuration of d^5 (S = 5/2). The unexpectedly small value of C implies deviation from the nominal chemical formula. Actually, the values of B_{iso} for Sr and Mn sites are extraordinarily large while somewhat small for O site. Refinements of the occupancies (g) for both the metal sites revealed no deviation from unity, and models with site splitting did not improve the fit between observed and the calculated patterns. Meanwhile, the simultaneous refinement of the g and B_{iso} parameters for O site were found unstable. To deal with this situation, several models including oxide defects and site splitting were examined. As a result, a model with mixed anions occupying the equatorial sites resulted in the most stable results (Fig. S1 and Table S1). The equatorial anion contents determined by the structural refinements was O:Cl = 0.88:0.12, and the B_{iso} value was 1.5(2) Å^2. The anion disorder may affect the atomic displacement parameters for the neighbouring cations. The Curie constant expected from the composition is 4.04 emu K/mol, which is still in disagreement with the re-estimated C value (Fig. S2). Neutron diffraction studies are needed to determine the anion contents and disordered states more accurately. The hysteresis observed at low temperatures is probably caused by some extrinsic effect such as impurities or defects in the magnetic planes. Indeed, the manganese oxychloride is very sensitive to air, which may damage the specimen during preparation for the magnetic measurements.

In summary, we demonstrated the high-pressure syntheses of new members of oxychloride perovskite compounds with a square-planar coordination, $Sr_2MnO_2Cl_2$, $Sr_2NiO_2Cl_2$ and $Ba_2PdO_2Cl_2$. In particular, square-planar coordinated Mn(II) and Ni(II) that are stabilized in a metal-anion array without any other kinds of metal cations are very rare among a number of extended transition metal compounds. We believe that further studies on the manganese and nickel oxychlorides deepen our understanding of the 2D magnetism in the $Sr_2MO_2Cl_2$ family.

This work was supported in part by the Japan Society for the Promotion of Science (JSPS) through a Grant-in-Aid for Scientific Research (25289233), and by the Funding Program for World-Leading Innovative R&D on Science and Technology (FIRST), Japan. The authors thank the staff of BL15XU, NIMS, for supporting the SXRD experiments (2013A4504, 2013B4503). YT thank K. Fujimaki and T. Taniguchi for support with the high-pressure synthesis at NIMS.

Notes and references

[a] Materials Processing Unit, National Institute for Materials Science (NIMS), 1-2-1 Sengen, Tsukuba, Ibaraki 305-0047, Japan.
[b] Superconducting Properties Unit, NIMS, 1-1 Namiki, Tsukuba, Ibaraki 305-0044, Japan.
[c] Materials Analysis Station, NIMS, 1-2-1 Sengen, Tsukuba, Ibaraki 305-0047, Japan.

†Electronic Supplementary Information (ESI) available: [details of any supplementary information available should be included here]. See DOI: 10.1039/b000000x/

1 E. Dagoto, *Rev. Mod. Phys.*, 1994, **66**, 763.
2 D. Vaknin, S. K. Sinha, C. Stassis, L. L. Miller and D. C. Johnson., *Phys. Rev. B*, 1900, **41**, 1926; Z. Hiroi, N. Kobayashi and M. Takano, *Nature*, 1994, **371**, 139.
3 L. L. Miller, X. L. Wang, S. X. Wang, C. Stassis, D. C. Johnston, J. Faber, Jr. and C.-K. Loong, *Phys. Rev. B* 1990, **41**, 1921.
4 B. J. Birgeneau, C. Y. Chen, D. R. Gabbe, H. P. Jenssen, M. A. Kastner, C. J. Peters, P. J. Picone, T. Thio, T. R. Thurston and H. L. Tuller, *Phys. Rev. B*, 1987, **59**, 1329; V. B. Grande, Hk. Müller-Buschbaum and M. Schweizer, *Z. Anorg. Allg. Chem*,. 1977, **428**, 120.
5 H. Manaka, T. Koide, T. Shidara and I. Yamada, *Phys. Rev. B*, 2003, **68**, 184412.
6 C. S. Knee and M. T. Weller, *J. Mater. Chem*., 2003, **13**, 1507; G. Corbel, J. P. Attfield, J. Hadermann, A. M. Abakumov, A. M. Alekseeva, M. G. Rozova and E. V. Antipov, *Chem. Mater.*, 2003, **15**, 189; R. L. Fuller and M. Greenblatt, *J. Solid State Chem*., 1991, **92**, 386.
7 T. Sowa, M. Hiratani and K. Miyauchi, *J. Solid State Chem*., 1990, **84**, 178.
8 T. Baikie, E. L. Dixon, J. F. Rooms, N. A. Young and M. G. Francesconi, *Chem. Commun.*, 2003, 1580; T. Baikie, M. S. Islam and M. G. Francesconi, *J. Mater. Chem.*, 200, **15**, 119.
9 C. S. Knee and M. T. Weller, *J. Solid State Chem.*, 2002, **168**, 1; C. S. Knee and M. T. Weller, *Phys. Rev. B*, 2004, **70**, 144406.
10 E. Dixon and M. A. Hayward, *Inorg. Chem.*, 2010, **49**, 9649; F. D. Romero, L. Coyle and M. A. Hayward, *J. Am. Chem. Soc.*, 2012, **134**, 15946.
11 Y. Tsujimoto, J. J. Li, K. Yamaura, Y. Matsushita, Y. Katsuya, M. Tanaka, Y. Shirako, M. Akaogi and E. Takayama-Muromachi, *Chem. Commun.*, 2011, **47**, 3263; Y. Tsujimoto, K. Yamaura and T. Uchikoshi, *Inorg. Chem.*, 2013, **52**, 10211.
12 H. Wu, *Eur. Phys. J. B*, 2002, **30**, 501.
13 N. McGlothlin, D. Ho and R. J. Cava, *Mat. Res. Bull.*, 2000, **35**, 1035.
14 M. Tanaka, Y. Katsuya, Y. Matsushita and O. Sakka, *J. Cera. Soc. Jpn.*, 2013, **121**, 287.
15 F. Izumi and K. Momma, *Solid State Phenom.*, 2007, **130**, 15.
16 R. D. Shannon, *Acta Cryst.*, 1976, **A32**, 751.
17 K. Shiro, I. Yamada, N. Ikeda, K. Ohgushi, M. Mizumaki, R. Takahashi, N. Nishiyama, T. Inoue and T. Irifune, *Inorg. Chem.*, 2013, **52**,1604; W. Yi, Y. Matsushita, M. Tanaka and A. A. Belik,

Inorg. Chem., 2012, **51**, 7650; V. H. Meyer and Hk. Müller-Buschbaum, *Z. Anorg. Allg. Chem.*, 1978, **442**, 26.

18 J. K. Kissick, C. Greaves, P. P. Edwards, V. M. Cherkashenko, E. Z. Kurmaev, S. Bartkowski and M. Neumann, *Phys. Rev. B*, 1997, **56**, 2831.

19 M. S. Kaluzhskikh, S. M. Kazakov, G. N. Mazo, S. Y. Istomin, E. V. Antipov, A. A. Gippius, Y. Fedotov, S. I. Bredikhin, Y. Liu, G. Svensson and Z. Shen, *J. Solid State Chem.*, 2011, **184**, 698.

20 M. Al-Mamouri, P. P. Edwards, C. Greaves and M. Slaski, *Nature*, 1994, **369**, 382.

21 K. G. Srivastave, *Phys. Lett.*, 1963, **4**, 55.

Journal Name

RSCPublishing

COMMUNICATION

New Members of Layered Oxychloride Perovskites with Square Planar Coordination: $Sr_2MO_2Cl_2$ (M = Mn, Ni) and $Ba_2PdO_2Cl_2$

Cite this: DOI: 10.1039/x0xx00000x

Received ooth January 2012,
Accepted ooth January 2012

DOI: 10.1039/x0xx00000x

www.rsc.org/

Y. Tsujimoto[a] C. I. Sathish[b] Y. Matsushita[c] K. Yamaura[b] and T. Uchikoshi[a]

New members of Ruddlesden-Popper type layered oxychloride compounds, $Sr_2MO_2Cl_2$ (M = Mn, Ni) and $Ba_2PdO_2Cl_2$, were synthesized under high-pressure conditions. Synchrotron XRD analysis revealed that all the phases adopt the tetragonal space group *I*4/*mmm*, where two-dimensional sheets composed of corner-sharing MO_4/PdO_4 squares were separated by rock-salt SrCl/BaCl layers.

Among many types of coordination geometries, square planar coordination has particularly received considerable attention from the perspective of superconductivity and low-dimensional magnetism.[1] $Sr_2CuO_2Cl_2$ is not only an ideal two-dimensional (2D) quantum Heisenberg antiferromagnet but also a parent compound of high-T_c superconductors.[2] $Sr_2CuO_2Cl_2$ is a Ruddlesden-Popper (R-P) type layered perovskite with the tetragonal K_2NiF_4 structure (space group *I*4/*mmm*).[3] As shown in Fig. 1 (a), the CuO_2 plane is alternately stacked with double rock-salt SrCl layers along the *c* axis. More specifically, the copper atom is loosely bound to the apical halogen atoms, but the copper coordination geometry can be viewed as a CuO_4 square due to the significantly elongated Cu–Cl bonds. The crystal symmetry is maintained down to low temperatures,[3] in sharp contrast to isostructural compounds (*T*-type) La_2CuO_4 and K_2CuF_4 showing an orthorhombic distortion below 530 K[4] and an cooperative orbital ordering of $d(x^2–r^2)/d(y^2–r^2)$[5], respectively. To date, many kinds of layered oxyhalide compounds analogous to R-P type structure have been reported; however, the variety of elements in square planar coordination is limited to Cu(II) with Jahn-Teller (J-T) effects and Pd(II) in a low-spin d^8 configuration with large crystal-field splitting energy.[6, 7, 8] Nevertheless, recent developments in synthetic methods successfully extended oxychloride systems with square-planar coordination to $Sr_2Co^{2+}O_2X_2$ (X = Cl, Br)[9] and $Sr_3M_2O_4Cl_2$ (M^{2+} = Fe, Co)[10] analogous to $Sr_2CuO_2Cl_2$ and $Ca_3Cu_2O_4Cl_2$[7], respectively.

High-pressure synthesis is a very useful technique to obtain new metastable phases that cannot be formed by conventional solid-state reaction. We recently synthesized new oxyhalide compounds Sr_2CoO_3F and Sr_2NiO_3X (X = F, Cl),[11] where the transition metal centres are surrounded with four oxygen at the equatorial sites and halogen/oxygen atoms at the apical sites (Fig. 1(c)). Similarly to $Sr_2CuO_2Cl_2$, these compounds have weak interaction between the transition metal centre and the halide ion, leading to formation of a distorted square pyramid with the surrounding oxide ions.[12] As seen in $Sr_2CoO_2Cl_2$ and Sr_2CoO_3Cl, full filling of apical sites with halide ions allows to change coordination environment around the metal centre from square pyramid to square plane.[9, 13] However, only two examples are known in the $Sr_2MO_2Cl_2$ (M = Co, Cu) family until now, which hampers systematic study of the 2D magnetism as a function of quantum spin number. Thus, preparation of another members of this family are highly demanded.

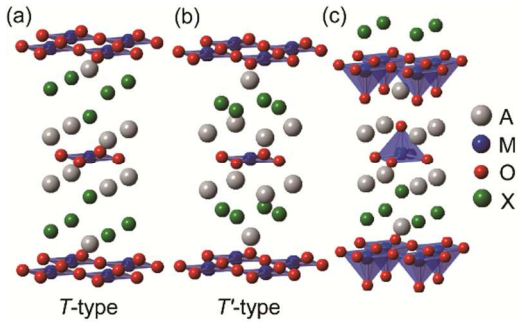

Fig. 1 Crystal structure of (a, b) $A_2MO_2X_2$ and (c) A_2MO_3X (A = rare earth, Alkali, Alkaline earth metal; M = transition metal; X = halogen).The structures of (a) and (b) are termed *T*-(La_2CuO_4) and *T*′-(Nd_2CuO_4) phases, respectively.

In this communication, we report new members of layered oxychloride compounds with a square planar coordination, $Sr_2MnO_2Cl_2$, $Sr_2NiO_2Cl_2$ and $Ba_2PdO_2Cl_2$, which are isostructural with $Sr_2CuO_2Cl_2$. All the present compounds were synthesized by a high-pressure and high-temperature method. Magnetic susceptibility measurements for the three compounds revealed characteristic magnetism reflecting their electronic structures: paramagnetic, antiferromagnetic (AFM) and diamagnetic behaviours for the manganese, nickel and palladium oxychloride compounds, respectively.

$Sr_2MnO_2Cl_2$, $Sr_2NiO_2Cl_2$ and $Ba_2PdO_2Cl_2$ were prepared from stoichiometric mixtures of in-house synthesized SrO_2, Mn (99.9 %)

and $SrCl_2$ (99.9%), SrO_2, Ni (99.9%) and $SrCl_2$, and BaO (99%), PdO (99.9%) and $BaCl_2$ (99.9%), respectively. Each mixture enclosed in a Pt capsule was heated for 1 h in a belt-type high-pressure apparatus at 3 GPa and 1400 °C for $Sr_2NiO_2Cl_2$ and $Ba_2PdO_2Cl_2$, and at 6 GPa and 1500 °C for $Sr_2MnO_2Cl_2$. After the treatment, the samples were quickly quenched to room temperature, and then the pressure was slowly released. The sample colour were black for $Sr_2MnO_2Cl_2$ and $Ba_2PdO_2Cl_2$, and dark green for $Sr_2NiO_2Cl_2$. Synchrotron powder X-ray diffraction (SXRD) data were collected at room temperature using a one-dimensional X-ray detector installed on BL15XU,[14] NIMS beamline at SPring-8. The wave length was λ = 0.65298 Å. The data were analysed by the Rietveld method with the program RIETAN-FP.[15] Magnetic susceptibilities were measured over the temperature range of T = 10−400 K in an applied magnetic field of H = 1 kOe for $Sr_2MnO_2Cl_2$ and $Sr_2NiO_2Cl_2$ and H = 10 kOe for $Ba_2PdO_2Cl_2$, using a superconducting quantum interference device (SQUID) magnetometer (Quantum Design, MPMS-XL).

Table. 1. Crystallographic data for $Sr_2MO_2Cl_2$ (M = Mn, Ni) and $Ba_2PdO_2Cl_2$ from Rietveld refinement of synchrotron X-ray diffraction data.

		$Sr_2MnO_2Cl_2$		$Sr_2NiO_2Cl_2$		$Ba_2PdO_2Cl_2$	
Atom	Site	z	B_{iso} (Å)	z	B_{iso} (Å)	z	B_{iso} (Å)
Sr/Ba	(0,0,z) 4*e*	0.38753(10)	1.93(3)	0.39320(7)	0.85(2)	0.38764(3)	0.667(9)
M	(0,0,0) 2*a*	–	1.82(8)	–	0.71(5)	–	0.315(13)
O	(0,1/2,0) 4*c*	–	0.2(1)	–	1.40(12)	–	0.81(7)
Cl	(0,0,z) 4*e*	0.1834(2)	0.76(6)	0.17994(17)	0.78(6)	0.18816(11)	1.03(2)
a (Å)		4.09669(2)		4.03896(4)		4.12886(1)	
c (Å)		14.99435(16)		15.09293(16)		16.80766 (4)	
R_{wp} (%)		1.56		1.46		4.25	
R_g (%)		7.65		5.63		3.13	
S		2.11		1.63		2.54	
M–O (Å)		2.04835(1)		2.01948(3)		2.06443(1)	
M–Cl (Å)		2.750(5)		2.716(3)		3.1625(19)	
Sr/Ba–O (Å)		2.6535(10)		2.5839(7)		2.7979(4)	
Sr/Ba–Cl×2 (Å)		3.0857(17), 3.060(5)		3.0619(11), 3.219(3)		3.1854(8), 3.353(2)	

Figures 2(a)−(c) show the SXRD patterns of $Sr_2MnO_2Cl_2$, $Sr_2NiO_2Cl_2$ and $Ba_2PdO_2Cl_2$, respectively. All the data could be readily indexed on the simple body-centred tetragonal cell. Close inspection of the data revealed a small number of tiny and broad additional peaks, which are likely assigned as impurity phases. The lattice parameters of the products are a = 4.09669(2) Å and c = 14.99435(16) Å for $Sr_2MnO_2Cl_2$, a = 4.03896(4) Å and c = 15.092923(16) Å for $Sr_2NiO_2Cl_2$, a = 4.12886(1) Å and c = 16.80766(4) Å for $Ba_2PdO_2Cl_2$. Structural refinements based on a model of $Sr_2CuO_2Cl_2$ (space group $I4/mmm$) immediately converged well. The refined crystallographic data, including the atomic coordinates, isotropic atomic displacement parameters (B_{iso}) and selected bond lengths are presented in Table 1.

Common to all the products, the transition metal centre is surrounded with four oxide ions at the equatorial sites and two chloride ions at the apical sites. However, the coordination environment of the transition metal centres can be viewed as a square plane within the 1st coordination sphere. For example, the inplane Mn−O bond length (2.0483 Å) agrees well with the sum of the ionic radii of O^{2-} (r = 1.4 Å) and Mn^{2+} in four-fold coordination (r = 0.66 Å), rather than in six-fold coordination (r = 0.83 Å).[16] In addition, the Mn−Cl bonds (2.750 Å) along the c axis are much longer than those expected from the simple ionic model. The bond ratio of Mn−Cl/Mn−O is 1.34, comparable to the corresponding value of 1.35 for $Sr_2CoO_2Cl_2$, but smaller than 1.44 for $Sr_2CuO_2Cl_2$ with a strong J-T active Cu^{2+} centre. Bond valence sums (BVS) calculated for the manganese site is 2.36, consistent with the nominal oxidation state of Mn(II). It is worth noting that contribution of the Mn−Cl bonds to the total BVS for the manganese is only 15%. Therefore, we can conclude that the manganese coordination is effectively square planar. Same is true for the nickel and palladium oxychlorides with the bond ratios of 1.34 and 1.53. The BVS values for the nickel and palladium sites are 1.77 and 2.01, and the contributions of Ni−Cl and Pd−Cl bonds to the total BVS for the transition metal centre are 16.8% and 4.8%. The larger bond ratio and weaker Pd−Cl apical interaction in $Ba_2PdO_2Cl_2$ than those in $Sr_2MO_2Cl_2$ (M = Mn, Ni) can be explained by the general trend that the crystal field energy is larger in 4*d* series than that in 3*d* series. In fact, the large crystal-field splitting between $4d_{xy}$ and $4d_{x^2-y^2}$ orbitals of Pd(II) exclusively gives the formation of four coplanar bonds, accompanied by a low-spin configuration with S = 0.[8, 17] Similarly, the isoelectronic configuration would be expected for the d^8 nickel centre in $Sr_2NiO_2Cl_2$; however, this is not the case because relatively weak crystal field of Ni(II) in the nickel oxychloride creates half-filled d_{xy} and $d_{x^2-y^2}$ orbitals, that is, a high-spin state with S = 1, as presented later.

The newly obtained oxychloride compounds crystallize in the T (La_2CuO_4) type structure, which is significantly different from related oxyfluoride compounds such as $Sr_2CuO_2F_2$ and $Ba_2PdO_2F_2$, with the T' (Nd_2CuO_4) type structure (Fig. 1(b)).[8, 18] In a series of Ln_2CuO_4 (Ln = lanthanide), a transformation from T to T' structure takes place with smaller Ln^{3+} cations than La^{3+}.[19] Our structural studies suggest that the ionic size of halide ion is also a key factor to affect the relative stabilities of the two structures. In fact, related oxychlorides/oxyfluorides exclusively adopt the T/T'-type structure. There is one exception that $Sr_2CuO_2F_{2+\delta}$, where fluorine atoms are additionally located in the apical sites, adopts the T structure.[20] The structural transformation is induced by a change in anion stoichiometry.

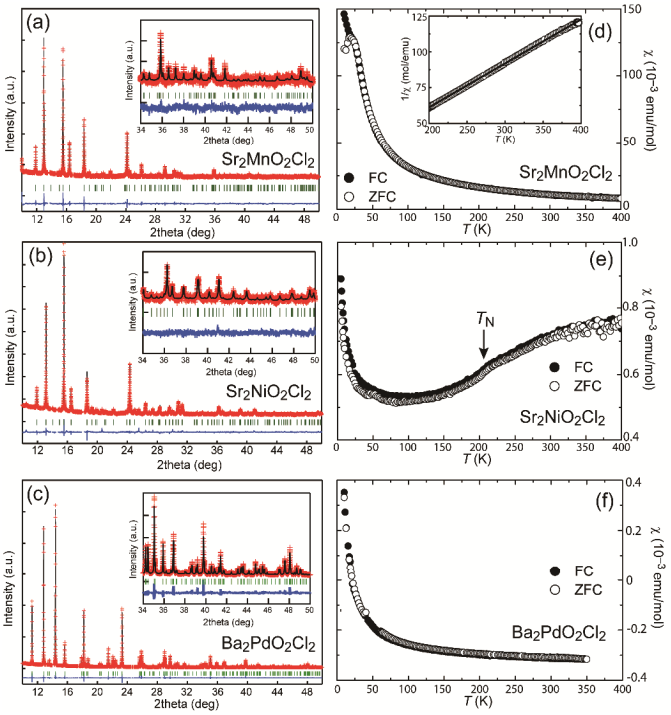

Fig. 2 (a)−(c) Observed (crosses), calculated (upper solid line), and difference (bottom solid line) plots from the Rietveld structural refinements against the synchrotron X-ray diffraction data collected from $Sr_2MnO_2Cl_2$, $Sr_2NiO_2Cl_2$ and $Ba_2PdO_2Cl_2$ at room temperature. Bragg reflections are indicated by vertical lines. The inset is a magnified view in a high 2θ region. (d)−(f) Magnetic susceptibilities (χ) measured under zero field cooled (open circles) and field cooled (solid circles) conditions. The inset shows the inverse susceptibility (open circles) and Curie-Weiss fit (solid line).

Figures 2(d)−(f) show the temperature dependence of the magnetic susceptibilities χ (= M/H) of the present compounds,

measured under zero-field cooled (ZFC) and field cooled (FC) conditions. The χ–T curve of $Ba_2PdO_2Cl_2$ shown in Fig. 2(f) exhibited a diamagnetic behaviour, indicating a d^8 low-spin configuration of Pd(II). A paramagnetic increase on cooling should be attributed to impurities or defects in the PdO_2 plane. In contrast, $Sr_2NiO_2Cl_2$, as shown in Fig. 2(e), displayed positive values over the measured temperature range and a gradual drop with decreasing temperatures from 400 K, indicative of 2D AFM correlation in the NiO_2 plane. The χ appears to take a maximum value at around 400 K ($\approx T^{\chi}_{max}$). In addition, a tiny cusp visible at T_N = 210 K is likely caused by a long-range magnetic ordering. Here, it is interesting to compare with a typical 2D antiferromagnet K_2NiF_4 with octahedrally coordinated nickel cations (T^{χ}_{max} = 250 K and T_N = 110 K).[21] The larger value of T^{χ}_{max} in the oxychloride underlies stronger superexchange interactions between the nearest neighbour nickel ions, which likely results from the square planar coordination of the nickel centre enhancing the orbital hybridization between nickel and ligands. Similarly to the nickel oxychloride, the manganese counterpart is expected to have AFM interactions within the MnO_2 plane. However, no sign of a long-range magnetic ordering was found in the χ of $Sr_2MnO_2Cl_2$ (Fig. 2(d)). Instead, it showed a paramagnetic behaviour down to 16 K, accompanied by a hysteresis between the ZFC and FC data. The Curie-Weiss fit to the data between 200 and 400 K gave C = 3.24 emu K/mol and θ = 1.5 K, where C and θ represent Curie constant and Weiss temperature, respectively. The estimated C value is much lower than a spin only value (4.37 emu K/mol) expected for Mn(II) in the high-spin configuration of d^5 (S = 5/2). The unexpectedly small value of C implies deviation from the nominal chemical formula. Actually, the values of B_{iso} for Sr and Mn sites are extraordinarily large while somewhat small for O site. Refinements of the occupancies (g) for both the metal sites revealed no deviation from unity, and models with site splitting did not improve the fit between observed and the calculated patterns. Meanwhile, the simultaneous refinement of the g and B_{iso} parameters for O site were found unstable. To deal with this situation, several models including oxide defects and site splitting were examined. As a result, a model with mixed anions occupying the equatorial sites resulted in the most stable results (Fig. S1 and Table S1). The equatorial anion contents determined by the structural refinements was O:Cl = 0.88:0.12, and the B_{iso} value was 1.5(2) Å^2. The anion disorder may affect the atomic displacement parameters for the neighbouring cations. The Curie constant expected from the composition is 4.04 emu K/mol, which is still in disagreement with the re-estimated C value (Fig. S2). Neutron diffraction studies are needed to determine the anion contents and disordered states more accurately. The hysteresis observed at low temperatures is probably caused by some extrinsic effect such as impurities or defects in the magnetic planes. Indeed, the manganese oxychloride is very sensitive to air, which may damage the specimen during preparation for the magnetic measurements.

In summary, we demonstrated the high-pressure syntheses of new members of oxychloride perovskite compounds with a square-planar coordination, $Sr_2MnO_2Cl_2$, $Sr_2NiO_2Cl_2$ and $Ba_2PdO_2Cl_2$. In particular, square-planar coordinated Mn(II) and Ni(II) that are stabilized in a metal-anion array without any other kinds of metal cations are very rare among a number of extended transition metal compounds. We believe that further studies on the manganese and nickel oxychlorides deepen our understanding of the 2D magnetism in the $Sr_2MO_2Cl_2$ family.

This work was supported in part by the Japan Society for the Promotion of Science (JSPS) through a Grant-in-Aid for Scientific Research (25289233), and by the Funding Program for World-Leading Innovative R&D on Science and Technology (FIRST), Japan. The authors thank the staff of BL15XU, NIMS, for supporting the SXRD experiments (2013A4504, 2013B4503). YT thank K. Fujimaki and T. Taniguchi for support with the high-pressure synthesis at NIMS.

Notes and references

[a] Materials Processing Unit, National Institute for Materials Science (NIMS), 1-2-1 Sengen, Tsukuba, Ibaraki 305-0047, Japan.
[b] Superconducting Properties Unit, NIMS, 1-1 Namiki, Tsukuba, Ibaraki 305-0044, Japan.
[c] Materials Analysis Station, NIMS, 1-2-1 Sengen, Tsukuba, Ibaraki 305-0047, Japan.

†Electronic Supplementary Information (ESI) available: [details of any supplementary information available should be included here]. See DOI: 10.1039/b000000x/

1 E. Dagoto, *Rev. Mod. Phys.*, 1994, **66**, 763.
2 D. Vaknin, S. K. Sinha, C. Stassis, L. L. Miller and D. C. Johnson., *Phys. Rev. B*, 1900, **41**, 1926; Z. Hiroi, N. Kobayashi and M. Takano, *Nature*, 1994, **371**, 139.
3 L. L. Miller, X. L. Wang, S. X. Wang, C. Stassis, D. C. Johnston, J. Faber, Jr. and C.-K. Loong, *Phys. Rev. B* 1990, **41**, 1921.
4 B. J. Birgeneau, C. Y. Chen, D. R. Gabbe, H. P. Jenssen, M. A. Kastner, C. J. Peters, P. J. Picone, T. Thio, T. R. Thurston and H. L. Tuller, *Phys. Rev. B*, 1987, **59**, 1329; V. B. Grande, Hk. Müller-Buschbaum and M. Schweizer, *Z. Anorg. Allg. Chem*,. 1977, **428**, 120.
5 H. Manaka, T. Koide, T. Shidara and I. Yamada, *Phys. Rev. B*, 2003, **68**, 184412.
6 C. S. Knee and M. T. Weller, *J. Mater. Chem*., 2003, **13**, 1507; G. Corbel, J. P. Attfield, J. Hadermann, A. M. Abakumov, A. M. Alekseeva, M. G. Rozova and E. V. Antipov, *Chem. Mater.*, 2003, **15**, 189; R. L. Fuller and M. Greenblatt, *J. Solid State Chem*., 1991, **92**, 386.
7 T. Sowa, M. Hiratani and K. Miyauchi, *J. Solid State Chem*., 1990, **84**, 178.
8 T. Baikie, E. L. Dixon, J. F. Rooms, N. A. Young and M. G. Francesconi, *Chem. Commun.*, 2003, 1580; T. Baikie, M. S. Islam and M. G. Francesconi, *J. Mater. Chem.*, 200, **15**, 119.
9 C. S. Knee and M. T. Weller, *J. Solid State Chem.*, 2002, **168**, 1; C. S. Knee and M. T. Weller, *Phys. Rev. B*, 2004, **70**, 144406.
10 E. Dixon and M. A. Hayward, *Inorg. Chem.*, 2010, **49**, 9649; F. D. Romero, L. Coyle and M. A. Hayward, *J. Am. Chem. Soc.*, 2012, **134**, 15946.
11 Y. Tsujimoto, J. J. Li, K. Yamaura, Y. Matsushita, Y. Katsuya, M. Tanaka, Y. Shirako, M. Akaogi and E. Takayama-Muromachi, *Chem. Commun.*, 2011, **47**, 3263; Y. Tsujimoto, K. Yamaura and T. Uchikoshi, *Inorg. Chem.*, 2013, **52**, 10211.
12 H. Wu, *Eur. Phys. J. B*, 2002, **30**, 501.
13 N. McGlothlin, D. Ho and R. J. Cava, *Mat. Res. Bull.*, 2000, **35**, 1035.
14 M. Tanaka, Y. Katsuya, Y. Matsushita and O. Sakka, *J. Cera. Soc. Jpn.*, 2013, **121**, 287.
15 F. Izumi and K. Momma, *Solid State Phenom.*, 2007, **130**, 15.
16 R. D. Shannon, *Acta Cryst.*, 1976, **A32**, 751.
17 K. Shiro, I. Yamada, N. Ikeda, K. Ohgushi, M. Mizumaki, R. Takahashi, N. Nishiyama, T. Inoue and T. Irifune, *Inorg. Chem.*, 2013, **52**,1604; W. Yi, Y. Matsushita, M. Tanaka and A. A. Belik,

Inorg. Chem., 2012, **51**, 7650; V. H. Meyer and Hk. Müller-Buschbaum, *Z. Anorg. Allg. Chem.*, 1978, **442**, 26.

18 J. K. Kissick, C. Greaves, P. P. Edwards, V. M. Cherkashenko, E. Z. Kurmaev, S. Bartkowski and M. Neumann, *Phys. Rev. B*, 1997, **56**, 2831.

19 M. S. Kaluzhskikh, S. M. Kazakov, G. N. Mazo, S. Y. Istomin, E. V. Antipov, A. A. Gippius, Y. Fedotov, S. I. Bredikhin, Y. Liu, G. Svensson and Z. Shen, *J. Solid State Chem.*, 2011, **184**, 698.

20 M. Al-Mamouri, P. P. Edwards, C. Greaves and M. Slaski, *Nature*, 1994, **369**, 382.

21 K. G. Srivastave, *Phys. Lett.*, 1963, **4**, 55.

